



Mechanism of reactivation of the peroxidase catalytic activity of human cyclooxygenases by reducing cosubstrate quercetin[☆]

Chengxi Yang ^{a,1}, Peng Li ^{a,1}, Pan Wang ^{a,b}, Bao Ting Zhu ^{a,b,*}

^a Shenzhen Key Laboratory of Steroid Drug Discovery and Development, School of Life and Health Sciences, The Chinese University of Hong Kong, Shenzhen 518172, China

^b Shenzhen Bay Laboratory, Shenzhen 518055, China

ARTICLE INFO

Keywords:

Quercetin
Cyclooxygenase
Peroxidase activity
Mechanism of enzyme activation

ABSTRACT

Our earlier studies show that the peroxidase activity of cyclooxygenase 1 and 2 (COX-1 and COX-2) can be reactivated in vitro and in vivo by the presence of certain naturally-occurring flavonoids such as quercetin and myricetin, which serve as reducing cosubstrates. These compounds can activate COX at nanomolar concentrations. In the present study, quercetin is used as a representative model compound to investigate the chemical mechanism by which the peroxidase activity of human COX-1 and COX-2 is reactivated after each catalytic cycle. Molecular docking and quantum mechanics calculations are carried out to probe the interactions of quercetin with the peroxidase sites of COX-1/2 and the reactivation mechanism. It is found that some of the partially-ionized states of quercetin can bind tightly and closely inside the peroxidase active sites of the COX enzymes and directly interact with heme Fe ion. While quercetin contains several phenolic hydroxyl groups, it is found that only the C-3'-OH group can effectively donate an electron for the reduction of heme because it not only can bind closely and tightly inside the peroxidase sites of COX-1/2, but it can also facilely donate an electron to heme Fe ion. This investigation provides a mechanistic explanation for the chemical process by which quercetin reactivates COX-1/2 peroxidases. This knowledge would aid in the rational design of drugs that can selectively target the peroxidase sites of COX-1/2 either as activators or inhibitors.

1. Introduction

Cyclooxygenases (COXs) catalyze the reaction from arachidonic acid (AA) to prostaglandin H₂ (PGH₂), which is further converted to prostaglandins (PGs), hydroxyeicosatetraenoic acids (HETEs), and thromboxanes, etc. [1–4]. There are two isoforms of COXs, i.e., COX-1 and COX-2. COX-1 is a ubiquitously expressed house-keeping enzyme in most tissues, but COX-2 expression is induced by inflammation and other pathological conditions [5].

There are two functionally-coupled catalytic sites in the COX-1/2 enzymes, namely, the cyclooxygenase site and the peroxidase site, and they catalyze two sequential reactions: the first reaction from AA to

prostaglandin G₂ (PGG₂), and the second reaction from PGG₂ to PGH₂ (Fig. S1) [6]. A branched model was proposed many years ago to link these two reactions together [6]. The peroxidase catalytic cycle is initiated through oxidation of the resting heme group (PPIXFe^{III}) which contains (proto)porphyrin and Fe ion to Compound I (i.e., the PPIX radical cation with an oxyferryl group attached to it, in the form of PPIX^{•+}Fe^{IV}=O). Next, Tyr385 donates one electron to Compound I, which becomes Compound II (PPIXFe^{IV}=O), a neutral PPIX with an oxyferryl group attached to it. Then the cyclooxygenase cycle is initiated by the Tyr385 radical, which converts AA to PGG₂ until “suicide inactivation” takes place. PGG₂ is then converted to PGH₂ in the peroxidase site while PPIXFe^{III} is oxidized to Compound I again [6–8,44,45].

Abbreviations: COX-1 and COX-2, cyclooxygenase 1 and 2, respectively; AA, arachidonic acid; PG, prostaglandin; PPIX, protoporphyrin IX; Por, porphyrin-imidazole complex.

[☆] This study is supported by research grants from the National Natural Science Foundation of China (NSFC No. 81473224 and No. 81630096), Shenzhen Key Laboratory Project (No. ZDSYS20190902093417963), Shenzhen Peacock Plan (No. KQTD2016053117035204), Shenzhen Bay Laboratory (No. SZB2019062801007).

* Corresponding author. School of Life and Health Sciences, The Chinese University of Hong Kong, 2001 Longxiang Road, Longgang District, Shenzhen, 518172, China.

E-mail address: btzhu@cuhk.edu.cn (B.T. Zhu).

¹ These two authors contributed almost equally to this study.

<https://doi.org/10.1016/j.jmgm.2021.107941>

Received 25 November 2020; Received in revised form 22 April 2021; Accepted 11 May 2021

Available online 28 May 2021

1093-3263/© 2021 Elsevier Inc. All rights reserved.

In our earlier study, some of the naturally-occurring flavonoids such as quercetin and myricetin were found to activate the peroxidase catalytic activity of COX-1/2 both in vitro and in vivo [9,10]. Notably, these compounds are effective at nM concentrations, which are physiologically relevant concentrations. Mechanistically, it is suggested that these compounds can bind inside the peroxidase active sites of COX-1/2 and donate electrons from their hydroxyl group(s) to the oxidized heme [10]. Accordingly, these compounds are considered reducing cosubstrates of COX-1/2 that can convert the oxidized heme group in the peroxidase active sites back to their resting state. However, the detailed catalytic mechanism by which natural reducing cosubstrates such as quercetin reactivate the peroxidase active sites is still not clear.

In the present study, molecular docking approach and quantum chemistry calculations are jointly used to study chemical mechanism by which quercetin (a selected representative flavonoid for investigation) serves as a reducing cosubstrate for the reactivation of the peroxidase activity of COX-1/2, i.e., how quercetin transfers its electron(s) to the oxidized heme for its reduction and thus reactivation of the peroxidase catalytic activity. Since quercetin has five hydroxyl groups in its structure (see Fig. 1), it is not known which hydroxyl group(s) is (are) capable of effectively donating an electron to COX-1/2, and finding an answer to this question is also a focus of this study.

2. Methods

2.1. Molecular docking

Energy minimization and molecular docking are performed with the Discovery Studio modeling software (Version 16.1.0.15350, Dassault Systèmes BIOVIA, San Diego, CA, U.S.A.) [11].

Protein structure refinement. The x-ray structure of human COX-1 (PDB code: 6y3c [12]) and human COX-2 (PDB code: 5kir [13]) are used as templates for computational docking analyses. All small molecules that are non-covalently attached to the COX proteins are removed, which include COX-1 (6y3c): chain A – FLC710, FLC711, FLC712 (citrate anion); chain B – NAG1, NAG2, BMA3, BMA4, BMA5 (oligosaccharides); chain C – NAG1, NAG2 (oligosaccharides); chain D – NAG1, NAG2 (oligosaccharides); and COX-2 (5kir): chain A – RCX601, NAG606, NH4607, GOL608, PO4609, PO4610, PO4611 (small molecules & oligosaccharides); chain C – NAG1, NAG2, MAN3 (oligosaccharides); chain D – NAG1, NAG2, MAN3 (oligosaccharides). Then the amino acid residues in the protein structures are renumbered according to the known sequences. The PPIX $^{Fe^{III}}$ component is individually added to the peroxidase sites of human COX-1 and COX-2. Notably, the reduced heme PPIX $^{Fe^{III}}$ (i.e., the resting state of heme) is contained in the original x-ray structures of COX-1 and COX-2, and is replaced with the

oxidized form of heme (in the form of PPIX $^{2+}Fe^{III}Fe^{IV}$ FeIVFeIV) for docking analysis of its binding interaction with the reducing cosubstrate. A similar approach was also used in a recent study that investigated the reactivation of COX-1/2 by phenol [15]. For preparation of the COX-1/2 proteins, the Prepare Protein module is used along with the CHARMM force field (version 22) [16].

Ligand processing. The C-3-O $^-$, C-5-O $^-$, C-7-O $^-$, C-3'-O $^-$ or C-4'-O $^-$ quercetin ion is created by removing a hydrogen atom in the respective hydroxyl group of quercetin. The 3D conformations of the quercetin molecules (listed in Fig. 1) are generated using the Prepare Ligand module which provides the starting structures for docking analysis.

Flexible docking. For flexible docking, the Find Sites from Receptor Cavities module is used to identify the binding sites in the prepared COX-1 and COX-2 structures. According to our earlier study, the target sites are the peroxidase active sites in these two COX enzymes [10]. For docking analysis, the active site near the peroxidase site and its SBD site Sphere are expanded to around 13 Å. All amino acid residues within a 5 Å reach of the target site are selected and allowed to have flexible side chains. Under the Flexible Docking mode with the maximum number of residues for creating side chain conformations set to 10, the Simulated Annealing docking method is then applied to dock quercetin into the target site of COX-1 and COX-2. Docking analyses are separately carried out for COX-1 and COX-2, with quercetin in both ionized and non-ionized states. Next the whole structure of each COX protein is further minimized with the CHARMM force field [14]. The suitability of the docking method was validated through performing the “self-docking” exercises as described in our recent study [15].

Calculation of binding energy. After completing flexible docking, the Calculate Binding Energy module is used to find complexes with the lowest binding energy value. The free energy of binding for a receptor-ligand complex is computed from the free energy of the complex, the target protein, and the ligand. The free energy values are separately computed using the CHARMM force field and the Poisson-Boltzmann equation with the non-polar surface area (PBSA) method [14,16]. In this approach, the Poisson-Boltzmann equation is solved numerically on a three-dimensional (3D) grid, and the computed electrostatic potential is used to estimate the electrostatic solvation free energy. The ligand conformational entropy is also taken into consideration during the free binding energy calculation. The following equation is used to calculate the binding energy ($\Delta G_{binding}$) between quercetin and the COX-1 or COX-2 protein:

$$\Delta G_{binding} = G_{complex} - (G_{COX} + G_{ligand})$$

where $G_{complex}$ is the absolute free energy of the complex, G_{COX} is the absolute free energy of the COX protein, and G_{ligand} is the absolute free energy of the ligand [17,18]. The $\Delta G_{binding}$ value is used to reflect the relative interaction affinity between the COX enzyme and the quercetin molecule.

The above docking analysis is carried out on a Windows Server R2 operating system on a Dell PowerEdge R730 workstation.

2.2. Quantum chemistry calculation of geometry and Gibbs free energy

The molecular geometry optimization and vibrational frequency calculation are performed on a Dell PowerEdge R730 workstation with GAUSSIAN 09W calculation software (Revision D.01, Gaussian, Wallingford, CT) [19].

Optimization of geometry. Geometrical structure and electronic information of different deprotonation states of quercetin are investigated using the B3LYP-D3 method (namely, the Becke's three-parameter hybrid functional and the Lee-Yang-Parr correlation functional method) [20–24], in combination of the IEFPCM model of water [25–27]. The 6-311+G(d,p) basis set is used for quercetin ions, while the 6-311G(d,p) basis set is used for non-ionized quercetin [28–31]. After the structures are optimized, the vibrational frequency is calculated. The

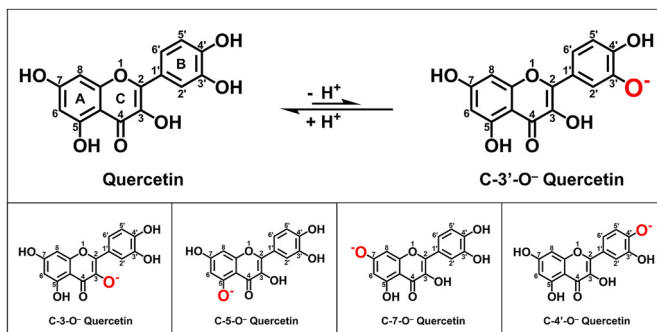


Fig. 1. Chemical structures of non-ionized quercetin and quercetin ions. Using the C-3'-OH group of quercetin as an example (as shown), it can undergo deprotonation (ionization). This deprotonation can also occur at quercetin's C-3-OH, C-5-OH, C-7-OH or C-4'-OH group. In this study, the deprotonation of a single hydroxyl group at C-3, C-5, C-7, C-3' or C-4' position is referred to as the partial ionization state.

coordinates of optimized structures are provided in Table S1. The calculated vibrational frequency values are used to aid in verifying the stationary points to be the real minimal values and also in obtaining thermal corrections at 310.00 K. Based on the computed optimized geometry of quercetin ions and their energy (E_-), the single point energy of the corresponding radicals (E_0^*) are calculated, thereby giving the vertical ionization potential (VIP) in the following equation:

$$VIP = E_0^* - E_-$$

The adiabatic ionization potential (AIP) of each quercetin ion is calculated through the energy of the optimized ion (E_-) and optimized radical (E_0) in the following equation:

$$AIP = E_0 - E_-$$

Density functional reactivity theory calculation. The nucleophilicity index (N) and the condensed local nucleophilicity index on O^- (N_{Nu}^0) for each quercetin ion are also calculated to compare the nucleophilicity of the O^- in different molecules [32]. Based on the optimized structure of quercetin ions, N and N_{Nu}^0 are calculated via the Multiwfns software [33] using the following equations:

$$N = E_{HOMO}(Nu) - E_{HOMO}(TCE)$$

$$N_{Nu}^0 = N \cdot f_O^-$$

where f_O^- is the condensed Fukui function on O^- [32,34]. These calculations are performed under the level of B3LYP/6-311G(d, p) [20–24, 28–31]. The $E_{HOMO}(TCE)$ is also evaluated using the same method and basis set.

3. Results and discussion

3.1. Binding of the first quercetin molecule inside the peroxidase sites of COX-1/2

Our recent study with phenol as a reducing cosubstrate show that when the peroxidase active sites of COX-1/2 have an oxygen atom covalently attached to the Fe^{IV} ion of heme (abbreviated as $PPIX^{•+}Fe^{IV}=O$), the reducing cosubstrate phenol fails to be docked closely inside the peroxidase active sites [15]. In this study, therefore, we first determine whether quercetin can be docked closely inside the peroxidase active sites when heme is in its oxidized form as $PPIX^{•+}Fe^{IV}=O$. Here it is of note that our recent studies [15,35,36] have shown that the binding interaction of a reducing cosubstrate inside the COX-1/2 peroxidase sites is strongly enhanced when the ligand is partially ionized. Therefore, in this study, docking analysis is also performed with both non-ionized and ionized quercetin molecules.

It is found that the binding energy values between $PPIX^{•+}Fe^{IV}=O$ and quercetin molecules in both non-ionized or ionized states are all positive, suggesting that the binding interactions are not favored energy-wise. Moreover, the distance between the hydroxyl O atoms of quercetin (i.e., when quercetin's C-3'-OH, C-4'-OH, C-3-OH, C-5-OH or C-7-OH is individually ionized) and heme Fe^{IV} ion is all longer than 5 Å for both ionized or non-ionized quercetin molecules (data not shown). Hence, it is apparent that the presence of the $Fe=O$ group in $PPIX^{•+}Fe^{IV}=O$ prevents the binding of both ionized and non-ionized quercetin molecules closely inside the peroxidase active sites.

Next, computational docking analysis is performed to determine whether quercetin in its non-ionized or ionized state can be docked inside the peroxidase active sites of COX-1/2 when the O atom is removed from the $Fe=O$ group (namely, in the form of $PPIX^{2+}Fe^{III}$). The binding

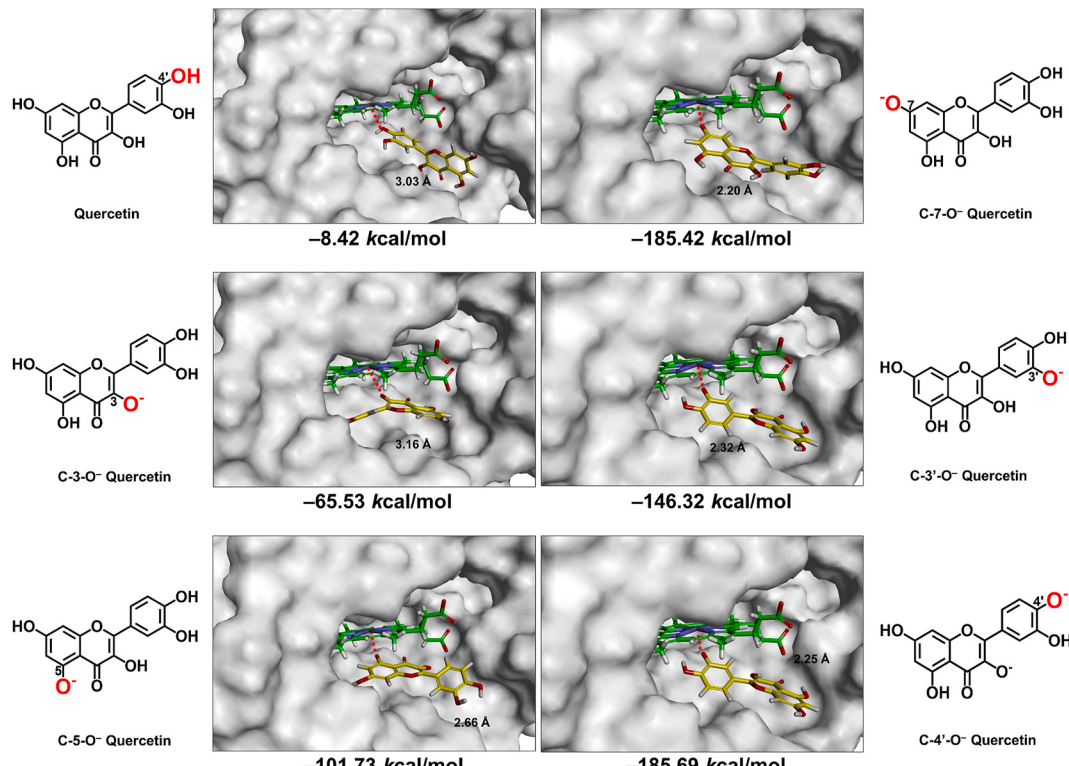


Fig. 2. Molecular docking analysis of the binding of non-ionized and partially-ionized quercetin inside the peroxidase active site of human COX-1 containing $PPIX^{2+}Fe^{III}$. The protein structure is shown as opaque gray surface. Carbon atoms in $PPIX^{2+}Fe^{III}$ are colored in green, nitrogen in blue, oxygen in red, hydrogen in white, and iron in black. Carbon atoms in quercetin molecule are colored in yellow, oxygen in red, and hydrogen in white. In addition, the dash line corresponds to the shortest distance between quercetin's phenolic oxygen atom and iron in $PPIX^{2+}Fe^{III}$. (For interpretation of the references to color in this figure legend, the reader is referred to the Web version of this article.)

energy for the best poses of non-ionized quercetin is -8.42 kcal/mol for COX-1 and -3.73 kcal/mol for COX-2, respectively, and the shortest distance between heme Fe ion and the hydroxyl O atoms is 3.03 Å for COX-1 and 9.72 Å for COX-2, respectively (Figs. 2 and 3, Table S1). The relatively high binding energy and long distance suggests that non-ionized quercetin cannot bind tightly and closely inside the peroxidase active sites of COX-1/2.

In comparison, when C-3'-O⁻, C-4'-O⁻, C-5-O⁻ or C-7-O⁻ quercetin ion (but not C-3-O⁻ quercetin ion) is individually analyzed, each molecule can be docked very closely to the heme Fe ion, with favorable binding energy levels (Figs. 2 and 3, Table S1). Taking C-3'-O⁻ quercetin ion as an example, its binding energy is -146.31 kcal/mol for COX-1 and -178.18 kcal/mol for COX-2 (Table S1), and its C-3'-O⁻ atom is very close to the heme Fe ion, with the Fe-O distance of 2.32 Å for COX-1 and 2.14 Å for COX-2, respectively (Table S1), which is sufficiently close for effective electron transfer. The zoom-in view of the binding interaction of C-3'-O⁻ quercetin ion inside COX-1's peroxidase site is shown in Fig. 4. The B-ring of C-3'-O⁻ quercetin ion is anchored very closely to heme, and it is suggested that multiple factors may contribute to this close interaction: a metal-acceptor interaction effect between the C-3'-O⁻ and Fe^{III}, a salt-bridge between the C-3'-O⁻ and His207, a hydrogen bond between C-4-OH and Gln203, and a Pi-Pi interaction between quercetin's B-ring and the porphyrin ring. Similar to C-3'-O⁻ quercetin, it is observed that the C-4'-O⁻, C-5-O⁻ or C-7-O⁻ quercetin can also bind inside the peroxidase active sites of COX-1/2, with favorable binding energy and acceptable Fe-O distance (Table S1, Figs. 2 and 3). By contrast, the binding interaction of C-3-O⁻ quercetin with COX-1/2 is weaker compared to all other ionization states, and its binding energy is higher and Fe-O distance is longer than 3 Å (Table S1, Figs. 2 and 3). The longer distance would make it almost impossible for electron transfer to take place.

Based on the results of the above docking analysis, it is apparent that ionized quercetin molecules (expect its C-3-O⁻ ion) generally can bind

far more favorably inside the peroxidase sites of COX-1/2 compared to non-ionized quercetin. This result is not surprising as similar observations were also made in our recent studies [15,35,36]. Based on the calculated pKa values of quercetin (summarized in Table 1), the extent of ionization of quercetin's five hydroxyl groups under physiologically-relevant pH conditions (pH 7.0–7.4) would vary considerably, and some of them (such as C-3'-OH) has a very low degree of ionization. However, based on results from quantum chemistry calculations (results described later), ionization of quercetin's C-3'-OH would be enhanced when it is bound inside the peroxidase active sites, thereby making this ionized form viable to serve as a reducing cosubstrate.

3.2. Transfer of the first electron from C-3'-O⁻ quercetin ion to heme

Our recent study with phenol as a reducing cosubstrate [15] shows that the O atom in the oxidized heme ($\text{Fe}^{\text{IV}}=\text{O}$) is removed first by two protons prior to binding with phenol and subsequent reduction of heme Fe ion [15]. It is suggested that quercetin may share the same mechanism of action as phenol, i.e., the O atom in the oxidized heme is removed first and then followed by reduction of heme Fe ion. The detailed process of proton-mediated cleavage of the $\text{Fe}=\text{O}$ bond resulting in O removal has been illustrated in our recent study, and this process takes place spontaneously without the participation of the reducing cosubstrate [15].

To probe how the electron is transferred from a reducing cosubstrate to heme Fe ion, computational models of several relevant intermediates [15], namely, $\text{Por}^{2+}\text{Fe}^{\text{III}}$, $\text{Por}^{\bullet+}\text{Fe}^{\text{III}}$ and $\text{Por}\text{Fe}^{\text{III}}$, have been established recently. These intermediates are identified based on the analysis of NBO charges, spin densities, and molecular orbital analyses [15]. In these models, PPIX is simplified into Por and the proximal His388 is simplified into imidazole ring (Im) to save computing time. Notably, this simplified model has also been used in earlier studies on cytochrome

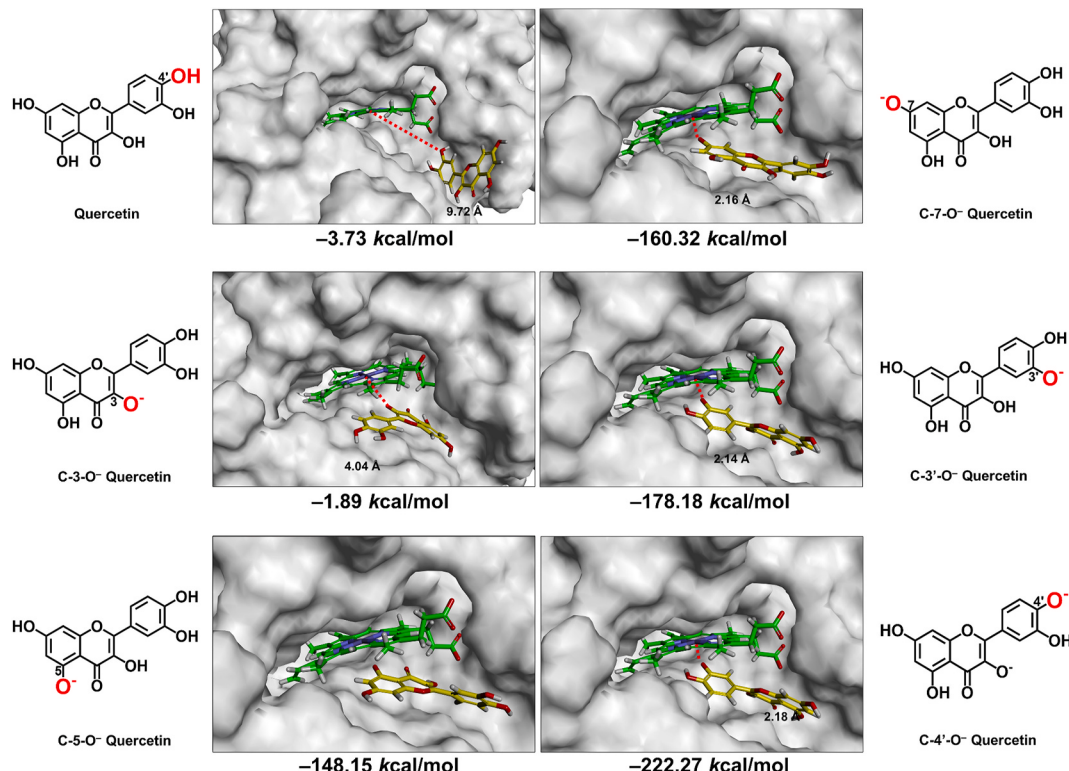


Fig. 3. Molecular docking analysis of the binding of non-ionized and partially-ionized quercetin inside the peroxidase active site of human COX-2 containing $\text{PPIX}^{2+}\text{Fe}^{\text{III}}$. The color labels are the same as Fig. 2. (For interpretation of the references to color in this figure legend, the reader is referred to the Web version of this article.)

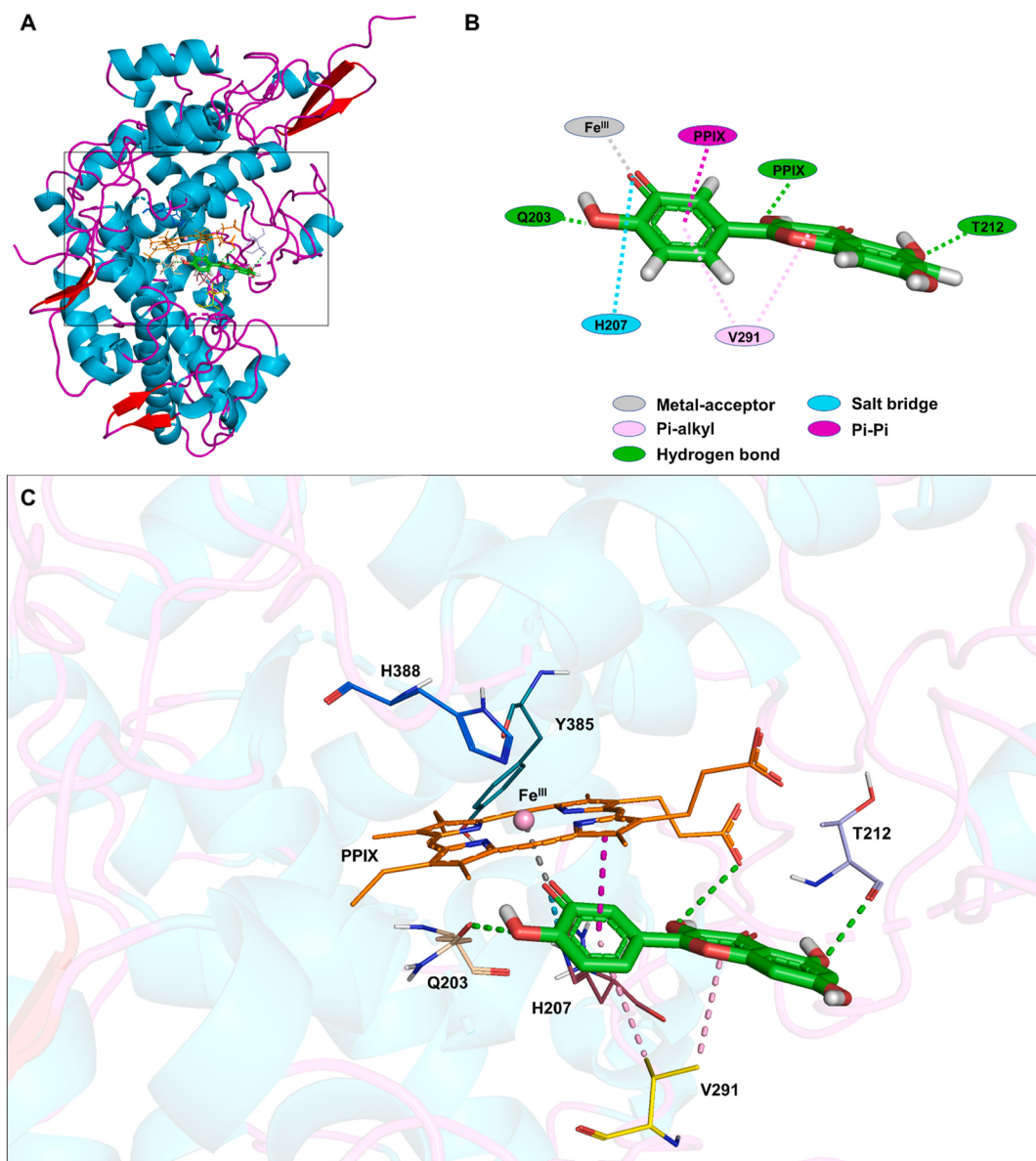


Fig. 4. Binding interactions of C-3'-O⁻ quercetin ion with amino acid residues inside the peroxidase active site of human COX-1 containing PPIX²⁺Fe^{III}. A. The structure of COX-1 in complex with C-3'-O⁻ quercetin ion and PPIX²⁺Fe^{III}. B. Two-dimensional (2D) interaction diagram of docked C-3'-O⁻ quercetin ion and key residues in the peroxidase active site of COX-1. C. The zoom-in view of C-3'-O⁻ quercetin ion inside the peroxidase site of COX-1 containing PPIX²⁺Fe^{III}. The protein structure is shown as solid ribbons, with different colors representing different types of the secondary structures in A and C. C-3'-O⁻ quercetin ion is shown as stick, with different colors representing different atomic elements. Fe^{III} is shown as sphere and colored in pink. All the nearby residues are shown in line, with PPIX²⁺ ring in orange, H388 in marine, Y385 in dark green, H207 in raspberry, V291 in yellow, Q203 in wheat, and T212 in light blue. All intermolecular interactions that facilitate the binding of C-3'-O⁻ quercetin ion are shown in dash lines, with metal-acceptor in gray, salt bridge in cyan, Pi-alkyl in pink, hydrogen bond in green, and Pi-Pi in magenta. (For interpretation of the references to color in this figure legend, the reader is referred to the Web version of this article.)

P450 enzymes [37–39]. Among the three intermediates, Por²⁺Fe^{III} is formed by the cleavage of oxygen of the Fe=O group in Compound I, with the help of two protons [15]; Por²⁺Fe^{III} is reduced to Por^{•+}Fe^{III} by a reducing cosubstrate; Por^{•+}Fe^{III} undergoes the second reduction and becomes PorFe^{III}, the resting state. The optimized structures and the free energy values of these intermediates have been calculated using Gaussian [15].

According to the proposed mechanism of COX-1/2 reactivation by quercetin (Scheme 1), two electrons are required to restore Por²⁺Fe^{III} to PorFe^{III}. To explain how the first electron is transferred from the oxygen atom of quercetin ion to Por²⁺Fe^{III}, quantum chemistry calculations are performed. Here quercetin C-3'-O⁻ ion is used as an electron donor to illustrate the process. (The reasons for selecting quercetin C-3'-O⁻ ion as a viable electron donor are provided in later section.) The Gibbs free

energy change of the first electron transfer is -8.84 kcal/mol for the formation of ¹Por²⁺Fe^{II}, -28.97 kcal/mol for ³Por^{•+}Fe^{III}, and -44.01 kcal/mol for ⁵Por^{•+}Fe^{III}, and -28.44 kcal/mol for ⁷Por^{•+}Fe^{III}, respectively (Scheme 2). Thus, the first reduction by C-3'-O⁻ quercetin is favorable thermodynamically for all multiplicities. Our recent study has shown that the donated electron would enter the a_{2u} orbital of Por²⁺Fe^{III} (to d_{yz} when ¹Por²⁺Fe^{II} is formed), and this electron transfer would reduce ²Por²⁺Fe^{III} to ¹Por²⁺Fe^{II} or ³Por^{•+}Fe^{III}, ⁴Por²⁺Fe^{III} to ⁵Por^{•+}Fe^{III}, and ⁶Por²⁺Fe^{III} to ⁷Por^{•+}Fe^{III} [15].

3.3. Binding of the second quercetin molecule inside the peroxidase sites of COX-1/2

After the first electron is transferred from the C-3'-O⁻ of a quercetin

Table 1

Nucleophilicity index ***N***, condensed local nucleophilicity index N_{Nu}^0 , ***AIP***, ***VIP***, and relative energy of different deprotonation states of quercetin.

	<i>N</i> (eV)	N_{Nu}^0 (eV)	<i>AIP</i> (eV)	<i>VIP</i> (eV)	<i>NBO</i> charge	relative energy (kcal/mol)	pKa
C-3-O ⁻ quercetin ion	8.76	1.38	5.10	5.26	-0.83	+8.33	10.29
C-5-O ⁻ quercetin ion	8.19	1.32	5.66	5.76	-0.78	0.00	7.85
C-7-O ⁻ quercetin ion	7.97	1.38	5.83	5.92	-0.80	+0.67	6.38
C-3'-O ⁻ quercetin ion	9.04	1.97	5.23	5.37	-0.87	+10.02	12.82
C-4'-O ⁻ quercetin ion	8.38	1.18	5.30	5.44	-0.83	+0.19	8.63

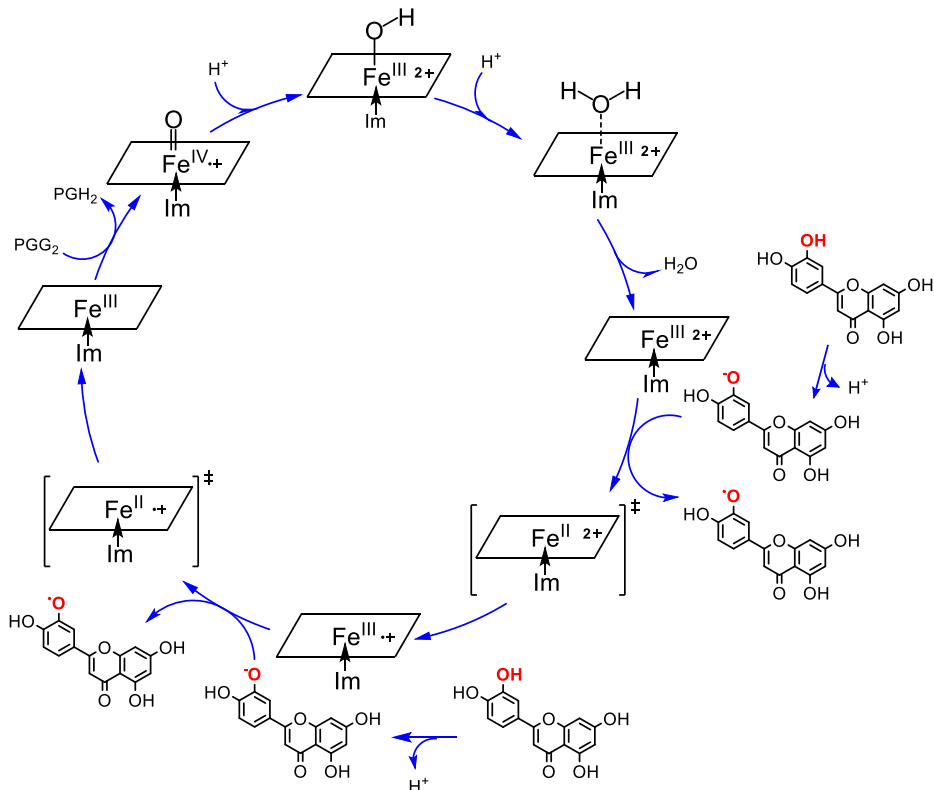
ion to PPIX²⁺Fe^{III} of COX-1/2, PPIX^{•+}Fe^{III} (or its singlet form PPIX²⁺Fe^{II}) is formed. Based on results from quantum chemistry calculations (discussed later), it is apparent that each quercetin molecule can actually only donate one electron from its C-3'-O⁻ ion for reduction of the peroxidase sites of COX-1/2. Next, a series of computations are performed to determine how the second quercetin molecule binds to the peroxidase sites of COX-1/2 and donates the second electron. Firstly, the Flexible Docking approach is used to dock the second quercetin molecule in its non-ionized and ionized states into the peroxidase active sites of COX-1/2 containing PPIX⁺Fe^{III} (Figs. 5 and 6). Non-ionized quercetin again cannot get close to the peroxidase sites of COX-1/2 and the shortest distance between heme Fe ion and the C-3' O atom is 4.27 Å for COX-1 and 10.11 Å for COX-2, respectively (Figs. 5 and 6, Table S1).

However, in the case of C-3'-O⁻ quercetin ion, its Fe–O distance is sufficiently short for electron transfer, at 2.33 Å for COX-1 and 2.22 Å for COX-2, respectively. Its relatively low binding energy suggests a favorable and tight binding interaction with the heme complex inside the peroxidase active sites. The zoom-in view of the binding interaction of C-3'-O⁻ quercetin with COX-1 is shown in Fig. 7. The A-ring of C-3'-O⁻ quercetin ion is close to Leu294 (4.00 Å), forming a Pi-alkyl interaction (Fig. 7C), which is different from the docking pose when the first quercetin C-3'-O⁻ ion is bound inside the peroxidase site (Fig. 4C). In addition, Gln203 forms two hydrogen bonds with quercetin C-3'-O⁻ ion: one with the O atom of C-3-OH (2.22 Å), and the other one with the O atom of C-3'-O⁻ (2.22 Å). It is of note that the binding energy for the second quercetin C-3'-O⁻ ion is higher than that for the first one, indicating that the second C-3'-O⁻ quercetin ion has a lower relative binding affinity than the first quercetin. This observation is expected since the second C-3'-O⁻ quercetin ion would bind to the heme complex which has a reduced overall positive charge. The same trend is also observed with C-7-O⁻ and C-4'-O⁻ quercetin ions.

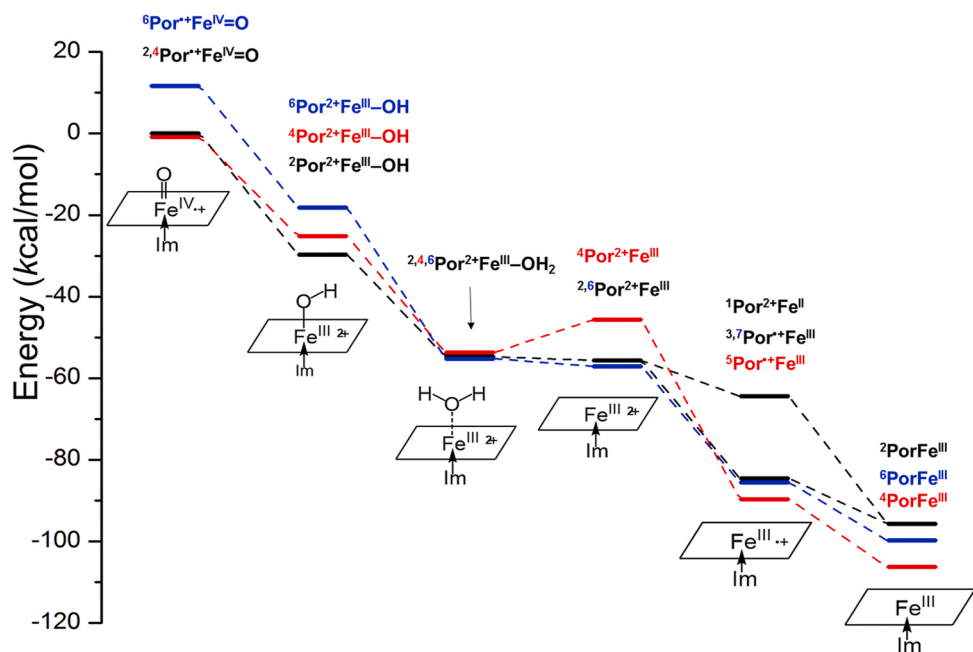
When the second quercetin molecule is docked inside the peroxidase sites, its C-3-O⁻ ion can interact with heme of COX-1 with a binding energy of -64.62 kcal/mol and the Fe–O distance of 2.16 Å (Table S2, Figs. 5 and 6). However, in the case of COX-2, the C-3-O⁻ quercetin ion displays a much weaker binding affinity (-1.02 kcal/mol) and longer Fe–O distance (4.04 Å). The binding energy of C-3-O⁻ quercetin ion for both COX-1/2 is markedly higher than that of C-7-O⁻, C-3'-O⁻ and C-4'-O⁻ quercetin ions, suggesting that the relative binding affinity of C-3-O⁻ quercetin ion is much weaker than that of C-7-O⁻, C-3'-O⁻ and C-4'-O⁻ quercetin ions.

3.4. Transfer of the second electron from C-3'-O⁻ quercetin ion to heme

Following the above docking analysis, the process of Por^{•+}Fe^{III} (Por²⁺Fe^{II} for singlet) reduction by the second electron is determined



Scheme 1. A proposed mechanism for the reactivation of the catalytic cycle of the COX-1/2 peroxidases by C-3-O⁻ quercetin ion. PPIX is shown as an abbreviated parallelogram, and the imidazole ring of His388 as Im. Also, PGG₂ is for prostaglandin G₂, and PGH₂ for prostaglandin H₂.



Scheme 2. The Gibbs free energy surface of the proposed cycle shown in Scheme 1.

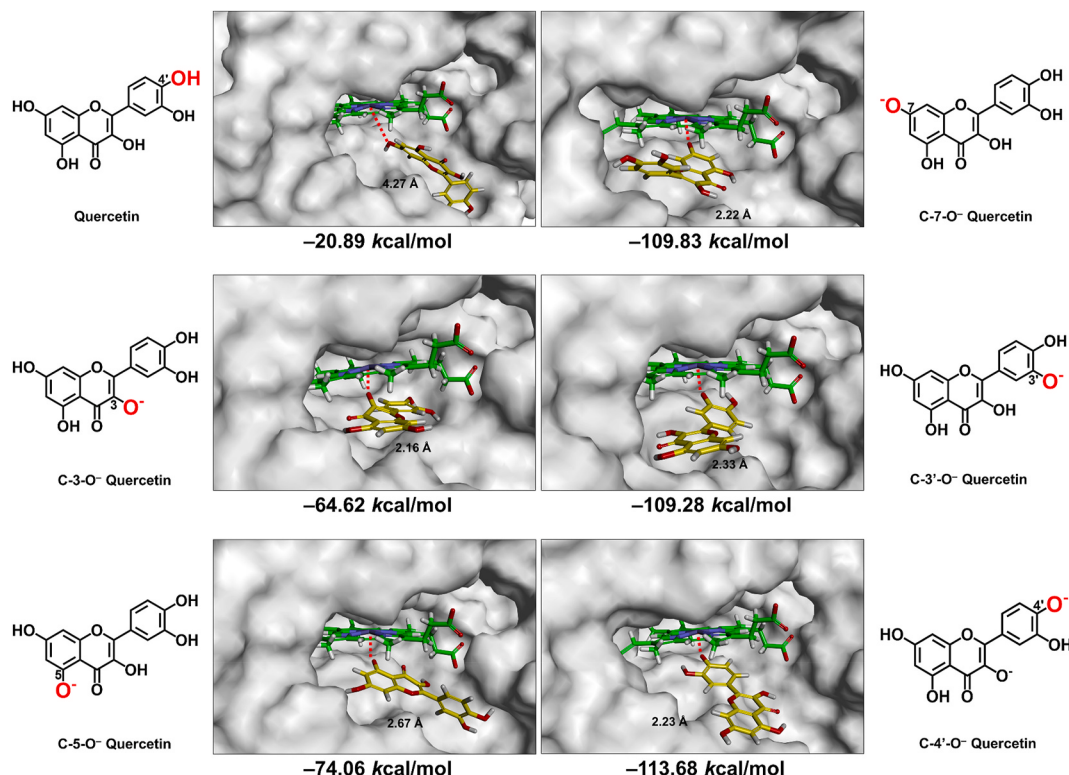


Fig. 5. Molecular docking analysis of the binding of non-ionized and partially-ionized quercetin inside the peroxidase active site of human COX-1 containing PPIX⁺ Fe^{III}. The color labels are the same as Fig. 2. (For interpretation of the references to color in this figure legend, the reader is referred to the Web version of this article.)

based on free energy calculations. It is found that the second reduction is also spontaneous, with a decrease in free energy by -11.08 , -11.62 and -14.28 kcal/mol for the formation of doublet, quartet and sextet Por-Fe^{III}, respectively. Combined with results from our recent study, the second electron transfer would reduce $^1\text{Por}^{2+}\text{Fe}^{\text{II}}$ to $^2\text{PorFe}^{\text{III}}$, $^3\text{Por}^{*+}\text{Fe}^{\text{III}}$ to $^2\text{PorFe}^{\text{III}}$, $^5\text{Por}^{*+}\text{Fe}^{\text{III}}$ to $^4\text{PorFe}^{\text{III}}$, and $^7\text{Por}^{*+}\text{Fe}^{\text{III}}$ to $^6\text{PorFe}^{\text{III}}$ (Scheme 2). More specifically, the electron from the second quercetin ion would

enter the a_{2u} orbital of the triplet, quintet, and septet of $\text{Por}^{*+}\text{Fe}^{\text{III}}$, thereby reducing heme to its resting state.

Details of the potential energy profiles for the regeneration of the peroxidase activity of COX-1 and COX-2 are assembled in Scheme 2. In general, three states of multiplicities of $\text{Por}^{*+}\text{Fe}^{\text{IV}}=\text{O}$ can all spontaneously go through the catalytic cycle in the presence of quercetin. While the quartet and doublet states at the beginning of the reaction cycle have

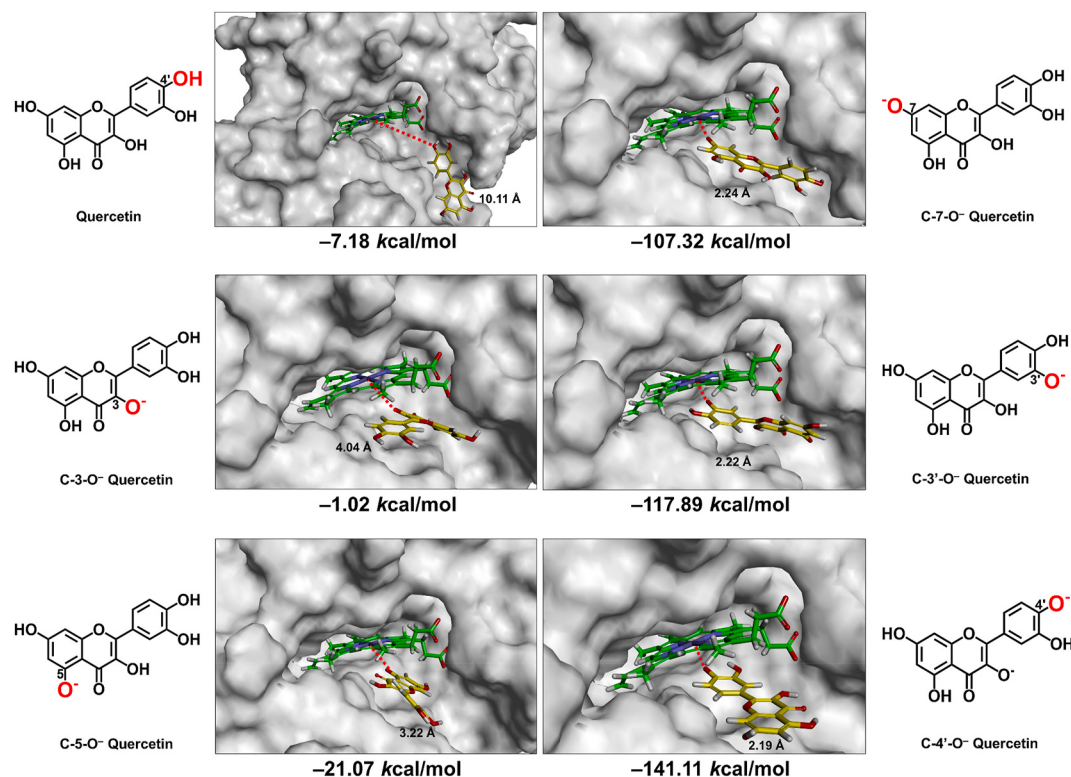


Fig. 6. Molecular docking analysis of the binding of non-ionized and partially-ionized quercetin inside the peroxidase active site of human COX-2 containing $\text{PPIX}^+ \text{Fe}^{\text{III}}$. The color labels are the same as Fig. 2. (For interpretation of the references to color in this figure legend, the reader is referred to the Web version of this article.)

relatively low energy levels compared to the energy level of the sextet state, the quartet state has the lowest energy in the last two reactions (**Scheme 2**). In comparison, the doublet state has the highest energy levels in the last two reactions. This information suggests that the quartet state likely is both more stable and thermodynamically more favored to proceed through the whole reaction cycle. **Scheme 2** also depicts several multiplicity shifts during the whole cycle, suggesting that recombination of electrons within the orbitals may be frequent in the cycle.

In **Scheme 1**, it is also proposed that electrons may not be directly transferred from quercetin ion to porphyrin, rather they are first transferred to Fe (Fe^{III} in $\text{Por}^{2+}\text{Fe}^{\text{III}}$ is reduced to Fe^{II} in $\text{Por}^{2+}\text{Fe}^{\text{II}}$) and then to porphyrin ($\text{Por}^{2+}\text{Fe}^{\text{II}}$ is converted to $\text{Por}^{\bullet+}\text{Fe}^{\text{III}}$). This hypothesis was first suggested in our recent study with phenol as a reducing cosubstrate [15], and it is supported by some of the computational results. It is postulated that the Fe ion has stronger electrophilicity compared to the porphyrin ring. ${}^1\text{Por}^{2+}\text{Fe}^{\text{II}}$, which is formed by direct electron transfer to Fe, displays a considerably higher energy level (about 22.46 kcal/mol higher) compared to ${}^3\text{Por}^{\bullet+}\text{Fe}^{\text{III}}$, ${}^5\text{Por}^{\bullet+}\text{Fe}^{\text{III}}$ and ${}^7\text{Por}^{\bullet+}\text{Fe}^{\text{III}}$. This relatively large energy difference between states of multiplicity is not observed in other groups of intermediates. ${}^1\text{Por}^{2+}\text{Fe}^{\text{II}}$ may serve as a reactive intermediate during the reduction and then undergo electron recombination to form ${}^3\text{Por}^{\bullet+}\text{Fe}^{\text{III}}$, ${}^5\text{Por}^{\bullet+}\text{Fe}^{\text{III}}$ or ${}^7\text{Por}^{\bullet+}\text{Fe}^{\text{III}}$. Therefore, it is postulated that the electrons are not transferred directly from the ionized reducing cosubstrate to porphyrin, instead they are firstly transferred to Fe and then to porphyrin.

3.5. Which hydroxyl group(s) of quercetin can effectively donate electron(s)?

As described above, the C-3'-O⁻, C-4'-O⁻, C-5-O⁻ or C-7-O⁻ quercetin ion each can bind inside the peroxidase active sites of COX-1/2 very closely to $\text{Por}^{2+}\text{Fe}^{\text{III}}$. Although each of these hydroxyl groups is electron-rich, it is not known which hydroxyl group(s) is/are actually capable of

donating an electron for the reduction of $\text{Por}^{2+}\text{Fe}^{\text{III}}$. The overall ability of a reducing cosubstrate is not only determined by its ability to bind tightly and closely inside the peroxidase active sites of COX-1/2, but it is also determined by its ability to effectively donate an electron for the reduction of heme.

To assess the ability of a reducing cosubstrate and its hydroxyl group(s) to donate an electron to heme Fe ion, a set of related parameters are jointly assessed in this study, which include the nucleophilicity index (*N*), condensed local nucleophilicity index (N_{Nu}^0), **NBO** charges, adiabatic ionization potential (**AIP**) and vertical ionization potential (**VIP**). The nucleophilicity index *N* evaluates the overall affinity of a molecule to an electrophile (i.e., the Fe ion of heme); the condensed local nucleophilicity index N_{Nu}^0 measures the affinity of each individual O⁻ in quercetin for an electrophile; and the **NBO** analysis mostly measures the amount of charge carried by each O⁻. As for **AIP** and **VIP**, both parameters reflect the level of energy increase in the reducing cosubstrate after it donates an electron, and accordingly, a reducing cosubstrate with lower **AIP** and **VIP** levels would mean that it can more facilely donate an electron.

As summarized in **Table 1**, C-3'-O⁻ quercetin has the highest nucleophilicity index *N* (9.04 eV), thus indicating that this quercetin ion has the highest affinity for binding to heme Fe ion compared to other quercetin ions. Also, C-3'-O⁻ quercetin ion has the highest value (1.97 eV), which indicates that the C-3'-O⁻ of quercetin has the highest affinity for heme Fe ion, and this O⁻ atom also bears the largest amount of negative charge as reflected by the lowest **NBO** value compared to other O⁻ atoms when each is individually deprotonated (**Table 1**). The combined results of N_{Nu}^0 and **NBO** analyses indicate a strong nucleophilicity of C-3'-O⁻, which coincides well with the results of nucleophilicity index *N*. In addition, the C-3'-O⁻ quercetin has the lowest levels of **AIP** (5.23 eV) and **VIP** (5.37 eV) compared to C-4'-O⁻, C-5-O⁻ and C-7-O⁻ quercetin ions, which can also bind favorably inside the peroxidase sites. Here it is of note that while C-3-O⁻ quercetin has even lower levels of **AIP** (5.10 eV) and **VIP** (5.26 eV) compared to C-3'-O⁻ quercetin, the longer distance

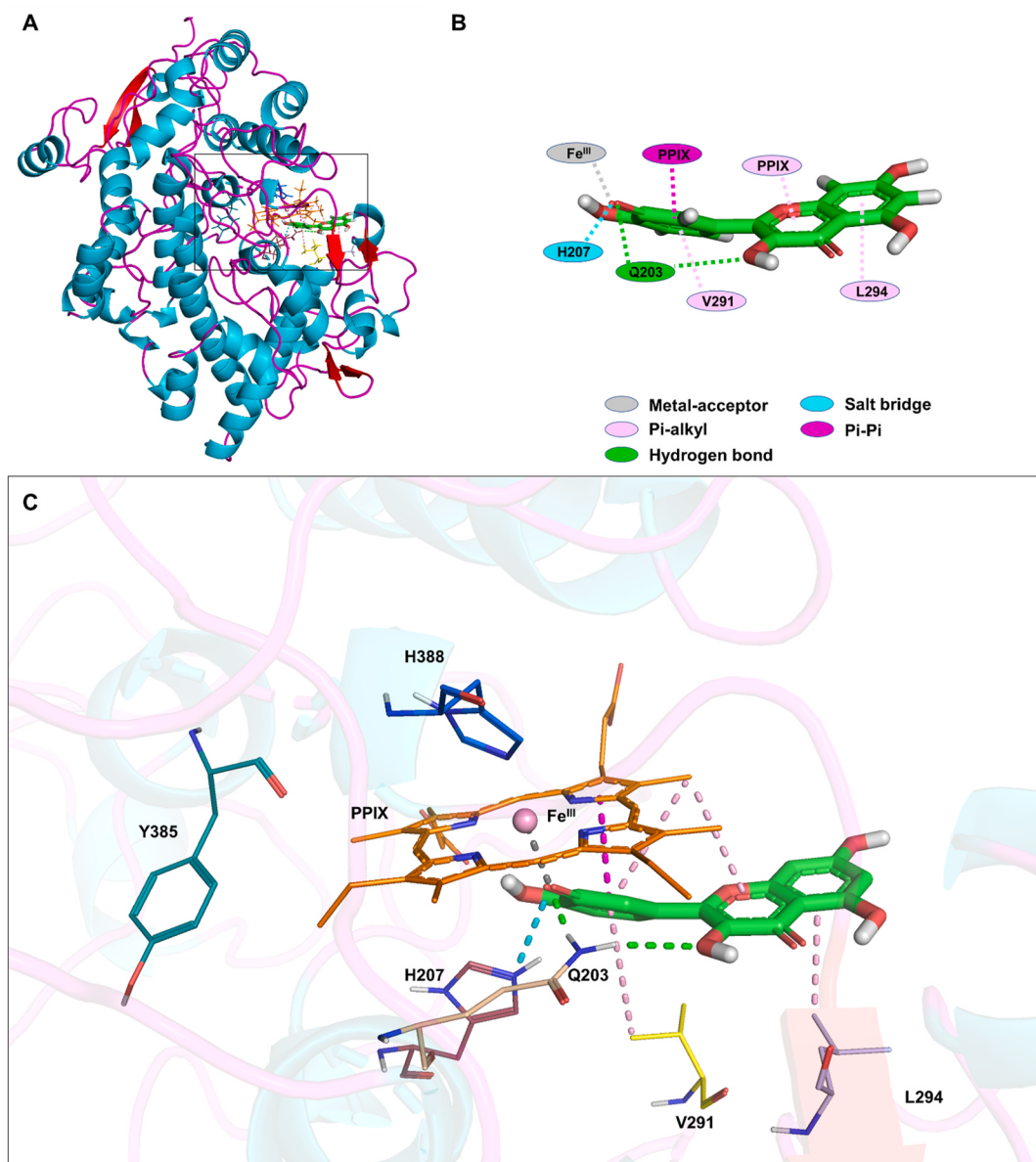


Fig. 7. Binding interaction of C-3'-O⁻ quercetin ion with amino acid residues inside the peroxidase active site of human COX-1 containing PPIX⁺ Fe^{III}. A. The structure of COX-1 in complex with C-3'-O⁻ quercetin ion and PPIX²⁺Fe^{III}. B. Two-dimensional (2D) interaction diagram of docked C-3'-O⁻ quercetin ion and key residues in the peroxidase active site of COX-1. C. The zoom-in view of C-3'-O⁻ quercetin ion inside the peroxidase site of COX-1. The protein structure is shown as solid ribbons, with different colors representing different types of the secondary structures in A and C. C-3'-O⁻ quercetin ion is shown as stick, with different colors representing different atomic elements. Fe^{III} is shown as sphere and colored in pink. All the nearby residues are shown in line, with PPIX⁺ ring in orange, H388 in marine, Y385 in dark green, H207 in raspberry, V291 in yellow, Q203 in wheat, and L294 in light blue. All intermolecular interactions that facilitate the binding of C-3'-O⁻ quercetin ion are shown in dash lines, with metal-acceptor in gray, salt bridge in cyan, Pi-alkyl in pink, hydrogen bond in green, and Pi-Pi in magenta. (For interpretation of the references to color in this figure legend, the reader is referred to the Web version of this article.)

from heme Fe ion to the oxygen atom of C-3-O⁻ makes C-3-O⁻ quercetin impossible to donate its electron. Together, it is apparent that among quercetin's multiple hydroxyl groups (C-3-O⁻, C-5-O⁻, C-7-O⁻, C-3'-O⁻ and C-4'-O⁻), the oxygen atom in C-3'-O⁻ has the highest ability to function as a reducing cosubstrate for the peroxidases of COX-1/2. This is because the C-3'-O⁻ quercetin ion not only binds more tightly inside the peroxidase sites of COX-1/2, but it also has a high potential to facilely donate an electron to heme Fe ion.

Here it is of note that our recent study shows that galangin, which shares the same structure as quercetin but lacks the C-3'-OH and C-4'-OH in its B-ring, basically lacks the ability to activate the catalytic activity of COX-1/2 both in vitro and in vivo [40]. This observation suggests that the three hydroxyl groups on the A- and C-rings (i.e., C-3-OH, C-5-OH

and C-7-OH) have little or no ability to effectively donate electrons. This experimental observation agrees well with the computational data presented in this study. As mentioned above, in the case of C-3-O⁻ quercetin, while it has the potential to donate an electron, but it fails to bind tightly and closely inside the peroxidase active sites of the enzymes. In the cases of the C-5-O⁻ and C-7-O⁻ quercetin ions, while they can bind favorably inside the peroxidase active sites, their overall ability for electron donation is far lower than C-3'-O⁻, making them virtually ineffective for electron donation. Lastly, when the overall electron-donating ability of C-4'-O⁻ quercetin ion is compared with that of other ineffective electron donors (i.e., the C-5-O⁻ and C-7-O⁻ quercetin ions), it is not difficult to conclude that the electron-donating ability of C-4'-O⁻ quercetin ion is not any better than those of C-5-O⁻

and C-7-O⁻ quercetin ions. Therefore, it is suggested that C-4'-O⁻ quercetin ion most likely is also an ineffective electron donor when it is bound inside the peroxidase active sites of the COX enzymes.

Based on all the information discussed above, it appears that only C-3'-O⁻ quercetin ion is capable of donating one electron when it is bound inside the peroxidase active sites of COX-1/2, and as such, two quercetin molecules are needed to complete the reactivation cycle of the peroxidase activity (Scheme 1). Here it is of note that when C-3'-O⁻ quercetin ion binds inside the peroxidase active sites of COX-1/2, the peroxidase activity would be reactivated; however, when any of the inactive quercetin ions are bound inside the peroxidase sites, the peroxidase activity would not be reactivated, instead the catalytic activity would be inactivated as the inactive quercetin ions would functionally serve as competitive inhibitors and their binding would prevent the binding of real reducing cosubstrate C-3'-O⁻ quercetin ion. The predicted dual activation-inhibition effect of different quercetin ions agrees well with our earlier experimental observations [9] showing that when the concentration of quercetin (or other structurally-similar reducing cosubstrates such as myricetin) increases, it displays a clear dual activation-inhibition effect on the peroxidase activity of COX-1/2 in vitro.

Lastly, it is of note that since quercetin's O⁻ ion at C-3' position is highly nucleophilic compared to the O⁻ ions at its C-4', C-3, C-5 and C-7 positions (discussed above), this might be the reason why C-3-OH's pKa is markedly higher than all other OH groups and also why C-3'-O⁻ quercetin ion has the highest energy compared to all other ions (Table 1). It is likely that quercetin's C-3'-O⁻ is so nucleophilic that it can easily bind with a proton (such as those contained in water), and this might explain why quercetin C-3'-O⁻ ion is only present in very small quantity in aqueous solution at pH 7.0–7.4 (estimated to be at 1.51–3.80 p.p.m.). Nevertheless, the C-3'-OH of quercetin may still be deprotonated when inside the peroxidase active sites of COX-1/2 due to the following reasons: (i) Analysis of the protein environment around the docked C-3'-O⁻ quercetin ion shows that most of the neighboring amino acid residues are basic or neutral, in favor of C-3'-OH ionization (Fig. S2). (ii) An earlier study showed that the distal His207 would facilitate the heterolytic cleavage of the O-H bond of hydroperoxide before it reacts with heme [41]. Similarly, docking analysis conducted in this study also shows that the O⁻ ion in quercetin's C-3' position can form a strong salt bridge with His207 (Figs. 4 and 7), which would help stabilize the C-3'-OH's deprotonation state. The results from present computational analysis are consistent with our earlier study showing that myricetin (an analog of quercetin) has little ability to activate the catalytic activity of the H207A mutant COX-2 [10], indicating that mutation of histidine to the nonpolar alanine can mostly abrogate the binding interaction of certain flavonoids with COX-2 as well as their ability to activate the enzyme.

The results of our present modeling study, while interesting and of value, also have certain limitations. In the docking analysis, the implicit solvent model was used to calculate the binding energy between quercetin and the COX enzymes. With this model, the degree of freedom of a system is reduced. Future similar studies may also consider the inclusion of the explicit solvent model for computing the binding energies [42]. Besides, the flexible docking approach which was applied in the present study to predict the protein-ligand binding interaction, might not fully represent the flexible and dynamic nature of the enzyme-substrate complexes [43]. Inclusion of detailed molecular dynamic (MD) simulations might help further corroborate the docking results.

Lastly, it is of note that the proposed two-step reduction mechanism may not be the only possible mechanism for quercetin-mediated activation of the COX enzymes. It might also be possible that one quercetin molecule, under certain circumstances, donates two electrons to the COX enzyme. Detailed QM/MM analyses [44,45] would aid in probing the reaction paths as well as the activation energy barriers of COX1/2-catalyzed reactions.

4. Conclusions

In the present study, by employing molecular docking and quantum chemistry calculation, we investigate the mechanisms by which quercetin molecule reactivates the peroxidase catalytic cycle of COX-1 and COX-2. Following oxygen removal in PPIX^{•+}Fe^{IV}=O by two sequential protons, two quercetin C-3-O⁻ ions are needed to bind in sequence inside the peroxidase sites of the enzymes, resulting in the reduction of PPIX²⁺Fe^{III} to its resting form PPIXFe^{III}, with each quercetin ion donating an electron. Among all five quercetin ions, only the C-3'-O⁻ ion is capable of donating an electron while inside the peroxidase active sites of COX-1/2, and accordingly, two quercetin molecules are needed to complete the reactivation cycle of the peroxidase activity. The results based on computational analysis of the binding interactions of quercetin inside the peroxidase sites of COX-1/2 are consistent with our earlier experimental observations [10]. The knowledge gained from this as well as our earlier studies [9,10,35,36] would aid in the design of structural analogs which can serve either as COX activators (i.e., they are capable of effectively donating electrons) or as competitive inhibitors (i.e., they can bind favorably inside of the peroxidase sites but cannot donate electrons).

Declaration of competing interest

The authors declare that they have no known competing interests or personal relationships that could have appeared to influence the work reported in this paper.

Appendix A. Supplementary data

Supplementary data to this article can be found online at <https://doi.org/10.1016/j.jmgm.2021.107941>.

References

- [1] M. Hamberg, B. Samuelsson, Oxygenation of unsaturated fatty acids by the vesicular gland of sheep, *J. Biol. Chem.* 242 (1967) 5344–5354.
- [2] T. Miyamoto, N. Ogino, S. Yamamoto, O. Hayashi, Purification of prostaglandin endoperoxide synthetase from bovine vesicular gland microsomes, *J. Biol. Chem.* 251 (1976) 2629–2636.
- [3] C.A. Rouzer, L.J. Marnett, Cyclooxygenases: structural and functional insights, *J. Lipid Res.* 50 (Suppl) (2009) S29–S34, <https://doi.org/10.1194/jlr.R800042-JLR200>.
- [4] L.J. Marnett, S.W. Rowlinson, D.C. Goodwin, A.S. Kalgutkar, C.A. Lanzo, Arachidonic acid oxygenation by COX-1 and COX-2. Mechanisms of catalysis and inhibition, *J. Biol. Chem.* 274 (1999) 22903–22906, <https://doi.org/10.1074/jbc.274.33.22903>.
- [5] R.G. Kurumbail, R.J. Kiefer, L.J. Marnett, Cyclooxygenase enzymes: catalysis and inhibition, *Curr. Opin. Struct. Biol.* 11 (2001) 752–760, [https://doi.org/10.1016/s0959-440x\(01\)00277-9](https://doi.org/10.1016/s0959-440x(01)00277-9).
- [6] L.J. Marnett, Cyclooxygenase mechanisms, *Curr. Opin. Chem. Biol.* 4 (2000) 545–552, [https://doi.org/10.1016/s1367-5931\(00\)00130-7](https://doi.org/10.1016/s1367-5931(00)00130-7).
- [7] G. Wu, C. Wei, R.J. Kulmacz, Y. Osawa, A.L. Tsai, A mechanistic study of self-inactivation of the peroxidase activity in prostaglandin H synthase-1, *J. Biol. Chem.* 274 (1999) 9231–9237, <https://doi.org/10.1074/jbc.274.14.9231>.
- [8] O.H. Callan, O.Y. So, D.C. Swinney, The kinetic factors that determine the affinity and selectivity for slow binding inhibition of human prostaglandin H synthase 1 and 2 by indomethacin and flurbiprofen, *J. Biol. Chem.* 271 (1996) 3548–3554, <https://doi.org/10.1074/jbc.271.7.3548>.
- [9] H.W. Bai, B.T. Zhu, Strong activation of cyclooxygenase I and II catalytic activity by dietary bioflavonoids, *J. Lipid Res.* 49 (2008) 2557–2570, <https://doi.org/10.1194/jlr.M800358-JLR200>.
- [10] P. Wang, H.W. Bai, B.T. Zhu, Structural basis for certain naturally occurring bioflavonoids to function as reducing co-substrates of cyclooxygenase I and II, *PloS One* 5 (2010), e12316, <https://doi.org/10.1371/journal.pone.0012316>.
- [11] Dassault Systèmes BIOVIA, Discovery Studio, Version 16.1.0.15350, Dassault Systèmes, San Diego, 2015.
- [12] Micciaccia, M., Belviso, B. D., Iaselli, M., Ferorelli, S., Perrone, M.G., Caliandro, R., & Scilimati, A. doi: 10.2210/pdb6Y3C/pdb (2020).
- [13] B.J. Orlando, M.G. Malkowski, Crystal structure of rofecoxib bound to human cyclooxygenase-2, *Acta Crystallogr. F Struct. Biol. Commun.* 72 (2016) 772–776, <https://doi.org/10.1107/S2053230X16014230>.
- [14] B.R. Brooks, et al., CHARMM: the biomolecular simulation program, *J. Comput. Chem.* 30 (2009) 1545–1614, <https://doi.org/10.1002/jcc.21287>.

- [15] C. Yang, P. Li, X. Ding, H.C. Sui, S. Rao, C.H. Hsu, W.P. Leung, G.J. Cheng, P. Wang, B.T. Zhu, Mechanism for the reactivation of the peroxidase activity of human cyclooxygenases: investigation using phenol as a reducing cosubstrate, *Sci. Rep.* 10 (2020) 15187, <https://doi.org/10.1038/s41598-020-71237-x>.
- [16] M. Feig, et al., Performance comparison of generalized born and Poisson methods in the calculation of electrostatic solvation energies for protein structures, *J. Comput. Chem.* 25 (2004) 265–284, <https://doi.org/10.1002/jcc.10378>.
- [17] U. Uciechowska, et al., Binding free energy calculations and biological testing of novel thiobarbiturates as inhibitors of the human NAD⁺ dependent histone deacetylase Sirt2, *Med. Chem. Commun.* 3 (2012) 167–173, <https://doi.org/10.1039/C1MD00214G>.
- [18] R. Pouplana, J.J. Lozano, J. Ruiz, Molecular modelling of the differential interaction between several non-steroidal anti-inflammatory drugs and human prostaglandin endoperoxide H synthase-2 (h-PGHS-2), *J. Mol. Graph. Model.* 20 (2002) 329–343, [https://doi.org/10.1016/s1093-3263\(01\)00133-4](https://doi.org/10.1016/s1093-3263(01)00133-4).
- [19] M.J. Frisch, et al., Gaussian 09 Rev. D.01. Gaussian 09, 2009.
- [20] A.D. Becke, Density-functional exchange-energy approximation with correct asymptotic behavior, *Phys. Rev. A Gen. Phys.* 38 (1988) 3098–3100, <https://doi.org/10.1103/physreva.38.3098>.
- [21] A.D. Becke, Density-functional thermochemistry. III. The role of exact exchange, *J. Chem. Phys.* 98 (1993) 5648, <https://doi.org/10.1063/1.464913>.
- [22] C. Lee, W. Yang, R.G. Parr, Development of the Colle-Salvetti correlation-energy formula into a functional of the electron density, *Phys. Rev. B Condens. Matter* 37 (1988) 785–789, <https://doi.org/10.1103/physrevb.37.785>.
- [23] P.J. Stephens, F.J. Devlin, C.F. Chabalowski, M.J. Frisch, Ab initio calculation of vibrational absorption and circular dichroism spectra using density functional force fields, *J. Phys. Chem.* 98 (1994) 11623–11627, <https://doi.org/10.1021/j100096a001>.
- [24] S. Grimme, J. Antony, S. Ehrlich, H. Krieg, A consistent and accurate ab initio parametrization of density functional dispersion correction (DFT-D) for the 94 elements H–Pu, *J. Chem. Phys.* 132 (2010) 154104, <https://doi.org/10.1063/1.3382344>.
- [25] S. Miertuš, E. Scrocco, J. Tomasi, Electrostatic interaction of a solute with a continuum. A direct utilization of ab initio molecular potentials for the revision of solvent effects, *Chem. Phys.* 55 (1981) 117–129, [https://doi.org/10.1016/0301-0104\(81\)85090-2](https://doi.org/10.1016/0301-0104(81)85090-2).
- [26] S. Miertuš, J. Tomasi, Approximate evaluations of the electrostatic free energy and internal energy changes in solution processes, *Chem. Phys.* 65 (1982) 239–245, [https://doi.org/10.1016/0301-0104\(82\)85072-6](https://doi.org/10.1016/0301-0104(82)85072-6).
- [27] J.L. Pascual-Ahuir, E. Silla, I. Tuñón, GEPOL: an improved description of molecular-surfaces. 3. A new algorithm for the computation of a solvent-excluding surface, *J. Comput. Chem.* 15 (1994) 1127–1138, <https://doi.org/10.1002/jcc.540151009>.
- [28] A.D. McLean, G.S. Chandler, Contracted Gaussian basis sets for molecular calculations. I. Second row atoms, Z= 11–18, *J. Chem. Phys.* 72 (1980) 5639, <https://doi.org/10.1063/1.438980>.
- [29] R. Krishnan, J.S. Binkley, R. Seeger, J.A. Pople, Self-consistent molecular orbital methods. XX. A basis set for correlated wave functions, *J. Chem. Phys.* 72 (1980) 650, <https://doi.org/10.1063/1.438955>.
- [30] T. Clark, J. Chandrasekhar, G.W. Spitznagel, P.V.R. Schleyer, Efficient diffuse function-augmented basis sets for anion calculations. III.† the 3-21+G basis set for first-row elements, Li–F, *J. Comput. Chem.* 4 (1983) 294–301, <https://doi.org/10.1002/jcc.54004040303>.
- [31] M.J. Frisch, J.A. Pople, J.S. Binkley, Self-consistent molecular orbital methods 25. Supplementary functions for Gaussian basis sets, *J. Chem. Phys.* 80 (1984) 3265, <https://doi.org/10.1063/1.447079>.
- [32] L.R. Domingo, E. Chamorro, P. Perez, Understanding the reactivity of captodative ethylenes in polar cycloaddition reactions. A theoretical study, *J. Org. Chem.* 73 (2008) 4615–4624, <https://doi.org/10.1021/jo800572a>.
- [33] T. Lu, F. Chen, Multiwfn, a multifunctional wavefunction analyzer, *J. Comput. Chem.* 33 (2012) 580–592, <https://doi.org/10.1002/jcc.22885>.
- [34] T. Lu, *Multiwfn Software Manual*, 3.100.12, Beijing Kein Research Center for Natural Sciences, 2019.
- [35] H.R. Wang, H.C. Sui, B.T. Zhu, Ellagic acid, a plant phenolic compound, activates cyclooxygenase-mediated prostaglandin production, *Exp. Ther. Med.* 18 (2019) 987–996, <https://doi.org/10.3892/etm.2019.7667>.
- [36] H.R. Wang, H.C. Sui, Y.Y. Ding, B.T. Zhu, Stimulation of the production of prostaglandin E₂ by ethyl gallate, a natural phenolic compound richly contained in Longan, *Biomolecules* 8 (2018), <https://doi.org/10.3390/biom8030091>.
- [37] S.P. de Visser, F. Ogliaro, N. Harris, S. Shaik, Multi-state epoxidation of ethene by cytochrome P450: a quantum chemical study, *J. Am. Chem. Soc.* 123 (2001) 3037–3047, <https://doi.org/10.1021/ja003544+>.
- [38] M. Filatov, N. Harris, S. Shaik, A theoretical study of electronic factors affecting hydroxylation by model ferryl complexes of cytochrome P-450 and horseradish peroxidase, *J. Chem. Soc. Perkin Trans. 2* (1999) 399–410, <https://doi.org/10.1039/A809385G>.
- [39] F. Ogliaro, S. Cohen, M. Filatov, N. Harris, S. Shaik, The high-valent compound of cytochrome P450: the nature of the Fe–S bond and the role of the thiolate ligand as an internal electron donor, *Angew. Chem. Int. Ed. Engl.* 39 (2000) 3851–3855, [https://doi.org/10.1002/1521-3773\(20001103\)39:21<3851::AID-ANIE3851>3.0.CO;2-9](https://doi.org/10.1002/1521-3773(20001103)39:21<3851::AID-ANIE3851>3.0.CO;2-9).
- [40] H.W. Bai, C. Yang, P. Wang, S. Rao, B.T. Zhu, Inhibition of cyclooxygenase by blocking the reducing cosubstrate at the peroxidase site: Discovery of galangin as a novel cyclooxygenase inhibitor, *Eur. J. Pharmacol.* 899 (2021), 174036.
- [41] L.M. Landino, B.C. Crews, J.K. Gierse, S.D. Hauser, L.J. Marnett, Mutational analysis of the role of the distal histidine and glutamine residues of prostaglandin-endoperoxide synthase-2 in peroxidase catalysis, hydroperoxide reduction, and cyclooxygenase activation, *J. Biol. Chem.* 272 (1997) 21565–21574, <https://doi.org/10.1074/jbc.272.34.21565>.
- [42] J. Zhang, H. Zhang, T. Wu, Q. Wang, D. van der Spoel, Comparison of implicit and explicit solvent models for the calculation of solvation free energy in organic solvents, *J. Chem. Theor. Comput.* 13 (3) (2017) 1034–1043.
- [43] Y.C. Chen, Beware of docking!, *Trends Pharmacol. Sci.* 36 (2) (2015) 78–95.
- [44] C.Z. Christov, A. Lodata, T.G. Karabencheva-Christova, S. Wan, P.V. Coveney, A. J. Mulholland, Conformational effects on the pro-s hydrogen abstraction reaction in Cyclooxygenase-1: an integrated QM/MM and MD study, *Biophys. J.* 104 (5) (2013) L5–L7.
- [45] J. Ainsley, A. Lodata, A.J. Mulholland, C.Z. Christov, T.G. Karabencheva-Christova, Combined quantum mechanics and molecular mechanics studies of enzymatic reaction mechanisms, *Adv. Protein Chem. Struct. Biol.* 113 (2018) 1–32.